



# Introduction to special issue: the *TransBrom Sonne* expedition in the tropical West Pacific

K. Krüger and B. Quack

GEOMAR Helmholtz Centre for Ocean Research Kiel, Kiel, Germany

Correspondence to: K. Krüger (kkrueger@geomar.de)

Received: 3 November 2011 – Published in Atmos. Chem. Phys. Discuss.: 13 January 2012

Revised: 24 July 2013 – Accepted: 9 August 2013 – Published: 25 September 2013

**Abstract.** This special section of Atmospheric Chemistry and Physics gives an overview of scientific results, collected during a West Pacific ship expedition in October 2009 with the Research Vessel (R/V) *Sonne*. The cruise focussed on chemical interactions between the ocean surface and the atmosphere above the tropical West Pacific and was planned within the national research project TransBrom ([www.geomar.de/~transbrom](http://www.geomar.de/~transbrom)). TransBrom aimed to particularly investigate very short lived bromine compounds in the ocean and their transport to and relevance for the stratosphere. For this purpose, chemical and biological parameters were analysed in the ocean and in the atmosphere, accompanied by a high frequency of meteorological measurements, to derive new insights into the multidisciplinary research field. This introduction paper presents the scientific goals and the meteorological and oceanographic background. The main research findings of the *TransBrom Sonne* expedition are highlighted.

## 1 Introduction

The ship cruise comprised a meridional cross-section through the tropical West Pacific from the northern mid-latitudes to the southern subtropics. The tropical West Pacific was chosen, because of the following scientific reasons: (1) the tropical West Pacific is thought to be an active source region for natural halocarbons (Yokouchi et al., 1999; Quack and Wallace, 2003; Butler et al., 2007); (2) only few marine halocarbon measurements exist in this ocean basin until now (<https://halocat.geomar.de>); (3) the atmosphere over the tropical West Pacific is convectively active throughout the year (Gettelman et al., 2002; Liu et al., 2007), enclosing

the main gate in the “Tropical Tropopause Layer” (TTL) for trace gases entering the stratosphere (Bonazzola and Haynes, 2004; Fueglistaler et al., 2005; Krüger et al., 2008; Montzka et al., 2011). The meridional transect through the West Pacific allows the investigation of halocarbon production, sea-air gas exchange and transport to the stratosphere in a coastal versus open ocean, tropical-extratropical, and hemispheric perspective.

Main goals were to measure marine and atmospheric halocarbon concentrations, to investigate their sources and emissions and to quantify their contribution to the stratospheric halogen loading and their ozone depletion potential (ODP). To achieve these objectives, the following studies were performed and are presented in this special issue and elsewhere:

1. Regular sea water and air sampling were carried out to analyse halocarbon distributions and sources, including different phytoplankton species (Quack et al., 2011). From these measurements halocarbon fluxes were derived for bromoform, dibromomethane and methyl iodide.
2. A global sea-to-air flux climatology for bromoform, dibromomethane and methyl iodide was created including the TransBrom data (Ziska et al., 2013) for the use in chemistry transport and chemistry climate models (Hossaini et al., 2013).
3. The TTL and the marine atmospheric boundary layer (MABL) were analysed across the West Pacific, using frequent radiosoundings. These measurements were also delivered to the Global Telecommunication System (GTS) of the World Meteorological Organization (WMO) to improve global meteorological

assimilations over the West Pacific, which are used as input data for the transport modelling.

4. The bromocarbon transport to the stratosphere is calculated with a Lagrangian approach, taking the observed flux of the brominated very short lived substances (VSLS) and their chemical degradation and washout into account in order to estimate their contribution to the stratospheric bromine loading and their ODP (Tegtmeier et al., 2012).
5. The iodine content was investigated: (a) within the MABL by applying reactive halogen measurements in and above the ocean surface (Großmann et al., 2013); (b) in the stratosphere based on trajectory calculations using observed in-situ methyl iodide fluxes (Tegtmeier et al., 2013).
6. First measurements of dimethyl sulfide (DMS) in the West Pacific were carried out (Zindler et al., 2013) to derive sea-air fluxes and to model the subsequent DMS transport to the TTL (Marandino et al., 2013).
7. Different instruments and methods were intercalibrated to compare in-situ reactive halogens from Multi-Axis Differential Optical Absorption Spectroscopy (MAX-DOAS) instruments and VSLS data from air canister samplings (Großmann et al., 2013; Brinckmann et al., 2012).
8. Ozone, carbon monoxide, and other trace gases were measured throughout the entire troposphere to investigate its physical and chemical structure (Rex et al., 2012; Ridder et al., 2012).
9. Satellite retrievals of biological (phytoplankton) (Bracher, personal communication) and chemical (formaldehyde, nitrogen dioxide) compounds were validated by in-situ ship measurements over the West Pacific (Peters et al., 2012).

## 2 Cruise overview

The expedition started in Tomakomai, Japan (42° N, 142° E) on 9 October 2009, arriving in Townsville, Australia (19° S, 147° E) on 24 October 2009. The cruise was designed as a non-stop transit through the tropical West Pacific, directly sailing from Japan to Australia performing regular underway measurements of sea water properties and atmospheric parameters. A list of the data, instruments and sampling intervals can be found in Table 1 (see also Quack and Krüger, IFM-GEOMAR Cruise Report No. 37, 2010). Figure 1 shows the meridional cross section through the West Pacific from the northern extratropics to the southern subtropics. Although the cruise took place towards the weakening phase of the typhoon season, three tropical storms hit the

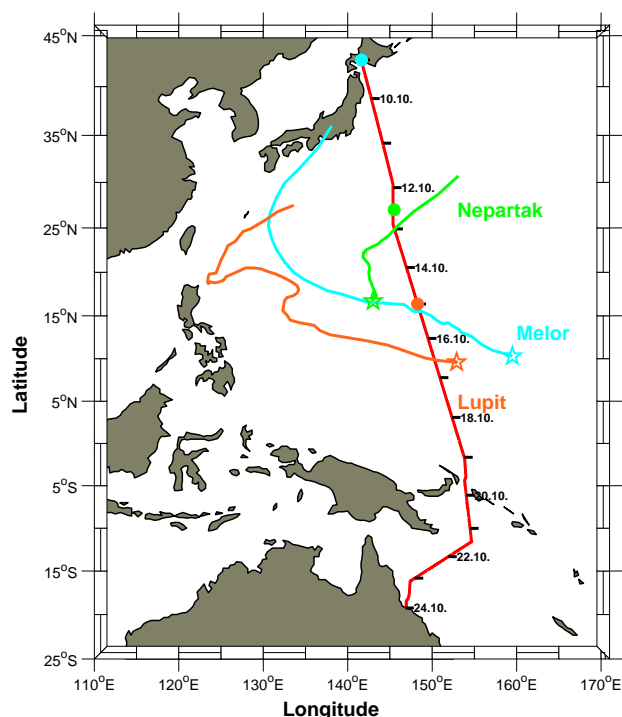


**Fig. 1.** *TransBrom Sonne* ship route in the West Pacific from 9 to 24 October 2009 (UTC time). The tracks from the tropical depression Nepartak and two typhoons Melor and Lupit are shown together with their localized influence on the ship measurements (filled circles). The data are taken from the Joint Typhoon Warning Centre archive (<http://www.usno.navy.mil/JTWC>).

R/V *Sonne* during the 16 day transit, influencing the trace gas content of the atmosphere by increasing their sea-to-air flux (Quack et al., 2011; Tegtmeier et al., 2012, 2013).

The ship departure was delayed by some hours due to the passage of the former super-typhoon Melor over Tomakomai on 8/9 October 2009, which turned into an extratropical storm while crossing Japan. Four days later, on 12 October 2009, the tropical storm Nepartak directly passed the ship route, leading to the wind maximum of the whole cruise at 27° N (Sect. 2.3). Again two days later (14 October 2009), the tropical storm Lupit developed at 12° N. While Nepartak was only categorised as a tropical depression (<http://www.usno.navy.mil/JTWC>), since it weakened when propagating northeastward (Fig. 1), Lupit turned into a super-typhoon of the category 4, travelling towards the Philippines. In addition to the tropical storm activity affecting the trace gas concentrations, we crossed the tropical West Pacific during the strengthening phase of an El Niño, which developed to a moderate-to-strong event during October 2009 (Climate Diagnostics Bulletin, 2009, 2010). In general, El Niño changes the oceanic and atmospheric circulations above the tropical Pacific, leading to an eastward shift of high sea surface temperature (SST), enhanced convection and transport to the stratosphere, impacting the production, sea-to-air

**Table 1.** Measurement table from the *TransBrom Sonne* cruise during October 2009. Data are stored at and can be requested from <https://portal.geomar.de/> (\* Quack and Krüger, IFM-GEOMAR Cruise Report No. 37, 2010).

Data	Instruments	Sampling	Contact	Publication
Cruise data	Ship sensors	1 s	B. Quack, GEOMAR	*
Meteorology	Ship sensors	1 s	B. Quack, GEOMAR	*
Oceanic halocarbons	GC-MS	3 h	B. Quack, GEOMAR	Quack et al. (2011), Ziska et al. (2013)
Oceanic DMS, DMSP, DMSO	GC-FPD	3 h	C. Zindler, GEOMAR	Zindler et al. (2013)
Oceanic N <sub>2</sub> O, CH <sub>4</sub>	GC-ECD, GC-FID	6 h	H. Bange, GEOMAR	*
Biological production and ocean optics:	HPLC, Flow cytometry, PSICAM, FRRF, RAMSES	3 h	A. Bracher, AWI	Zindler et al. (2013)
pCO <sub>2</sub> , dissolved O <sub>2</sub>	NDIR, Optode	1 min	A. Körtzinger, GEOMAR	*
Radiosoundings: meteorology, H <sub>2</sub> O, clouds, O <sub>3</sub>	Radio-/Snow-White/ COBALD/Ozone sondes	6 h/ samples 7/7/13	K. Krüger, GEOMAR	*
Atmospheric trace gases	Air canister, GC-MS	6 h	E. Atlas, RSMAS	Rex et al. (2012) Quack et al. (2011), Ziska et al. (2013)
Atmospheric ODS	Air canister, GC-MS	23 samples	A. Engel, GUF	Brinckmann et al. (2012)
Hydrogen isotopes	Air canister, CFIR-MS	60 samples	S. Walter, IMAU	*
BrO, IO	MAX-DOAS	15 min	K. Großmann, Univ HD	Großmann et al. (2013)
Reactive trace gases	MAX-DOAS	15 min	F. Wittrock, Univ B	Peters et al. (2012)
Major ions, Br, I	Ion chromatography	24 h	A. Baker, UEA	*
Aerosol optical depth	Sun photometer (Aeronet)	30 min	P. Croot, NUI Galway	*
Trace gas profiles	FTIR-spectrometer, -analyser	10 min	J. Notholt, Univ B	Ridder et al. (2012)
Bathymetry	Multibeam echosounder	Coral Sea	R. Beaman, JC Univ	*

The following acronyms stands for: GC-MS (Gas Chromatography-Mass Spectrometry), FPD (Flame Photometric Detector), ECD (Electron Capture Detector), FID (Flame Ionization Detector), HPLC (High Pressure Liquid Chromatography), PSICAM (Point-Source Integrating-Cavity Absorption Meter), FRRF (Fast Repetition Rate Fluorometer), RAMSES (Hyper spectral radiometer), NDIR (Non-Dispersive Infrared Detector), CFIR (Continuous Flow Isotopic Ratio), MAX-DOAS (Multi-Axis Differential Optical Absorption Spectroscopy), FTIR (Fourier Transform Infrared Spectroscopy), RSMAS (Rosenstiel School of Marine and Atmospheric Science), GUF (Goethe University Frankfurt), IMAU (Institute for Marine and Atmospheric research Utrecht), Univ HD (University Heidelberg), Univ B (University Bremen), UEA, (University of East Anglia), NUI (National University of Ireland), JC Univ (James Cook University).

gas exchange and transport of trace gases to the stratosphere (i.e. Bonazzola and Haynes, 2004; Krüger et al., 2008, 2009).

## 2.1 Data

Meteorological data, including air temperature, pressure and wind, were measured every second by the ship instruments at 20 m altitude. SST was recorded from 5 m depth in the hydrographic shaft, where 3-hourly sea surface water samples for halocarbon analysis were obtained. The halocarbon concentrations were analysed with a purge and trap gas chromatographic-mass spectrometric (GC-MS) system on board. Inter-calibration of the surface water and atmospheric concentrations was conducted with a National Oceanic and Atmospheric Administration (NOAA)-standard, obtained from the NOAA Earth System Research Laboratory in Boulder, Colorado, USA. Temperature, pressure and mean wind fields are displayed as 1 min and 10 min averages, respectively. Two different meteorological assimilations are analysed in more detail as they are used as data input for the transport studies, investigating the history of air parcels with trajectories (Sect. 3). The 4D-Var assimila-

tion of the operational European Centre for Medium Range Weather Forecast (opECMWF) model (cycle 35r3) is based on T799/L91 (~ 25 km) resolution (ECMWF Newsletter No. 121, 2009). If not specified, the opECMWF output is used with a 1° × 1° and 6-hourly resolution. The 3D-Var analysis of the operational National Centre for Environmental Prediction – Global Data Assimilation System (NCEP-GDAS) is based on T382/L64 (~ 35 km) resolution (NCEP Technical Procedures Bulletin, 2005), used with an average grid of 1° × 1° and 6-hourly data output.

## 2.2 Oceanographic background

Sea surface water and air temperatures are displayed in Fig. 2 to characterise the existing oceanographic circulation and to show their potential impact on the sea-air gas exchange. Trace gas emissions depend on water temperature and wind speed; at constant concentrations they increase with higher water temperatures and stronger wind speed (Wanninkhof, 1992; Nightingale et al., 2000).

At the beginning of the cruise, the ship passes the cold Oyashio current, when leaving Hokkaido Island southward.

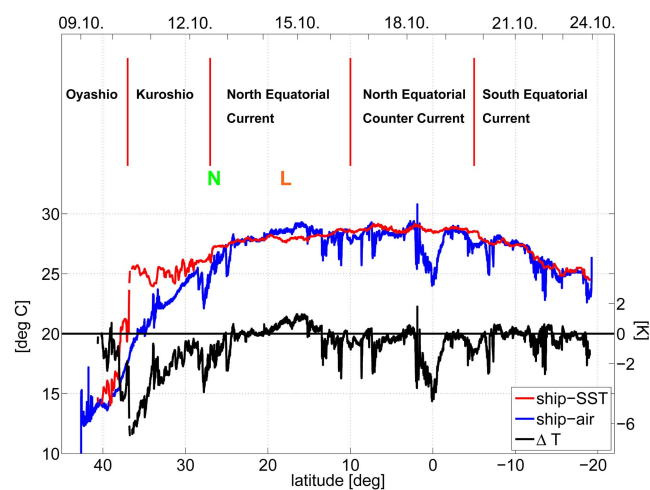


**Fig. 2.** Sea surface temperature ( $^{\circ}\text{C}$ ), surface air temperature ( $^{\circ}\text{C}$ ) and the difference between the two ( $\Delta T$ , in K) measured on board of R/V *Sonne* during October 2009. The measurements are displayed as 1 min averages. The identified oceanic circulations are displayed, as well as the influence of the tropical storms Nepartak (N) and Lupit (L).

The SST steadily increases from  $14^{\circ}\text{C}$  to  $21^{\circ}\text{C}$ . At  $38^{\circ}\text{N}$  a pronounced jump to higher SST indicates the transition to the Kuroshio current with water temperatures around  $25^{\circ}\text{C}$ . North Equatorial Current waters are characterised by a slight increase of SST up to  $28^{\circ}\text{C}$ , extending from  $28^{\circ}\text{N}$  to  $10^{\circ}\text{N}$ . Maximum SST of up to  $31^{\circ}\text{C}$ , hence the “warm pool” (SST  $> 28^{\circ}\text{C}$ ), is detected between  $10^{\circ}\text{N}$  and  $5^{\circ}\text{S}$ , within the region of the North Equatorial Counter Current. Monthly mean October maps revealed warmest surface water ( $>30^{\circ}\text{C}$ ) shifted further eastward towards the tropical Central to East Pacific, exceeding a moderate deviation of 1 K above the equator (Climate Diagnostics Bulletin, 2009). From  $6^{\circ}\text{S}$  to the end of the cruise in Townsville ( $19^{\circ}\text{S}$ ), the SST decreases to  $25^{\circ}\text{C}$  as the *Sonne* passed through the South Equatorial Current (Fig. 2). Most of the time the air temperature stays below the water temperature ( $\Delta T < 0\text{K}$ ), except between  $20^{\circ}\text{N}$  to  $15^{\circ}\text{N}$   $\Delta T > 1\text{K}$  due to the westward advection of warmer air from the Central Pacific (Sect. 3, Fig. 5). There is a sharp drop in  $\Delta T$  exceeding 7 K at the barrier between the Oyashio and the Kuroshio currents, when colder air masses from the North (Sect. 2.3) reach the warmer Kuroshio current.

### 2.3 Atmospheric background

During October 2009 the tropical convection and precipitation were enhanced over the central part of the tropical West Pacific, which is typical for a strengthening El Niño (Climate Diagnostics Bulletin, 2009). Indeed, our meteorology measurements on board revealed recurring convective activity within the inner tropical regime accompanied by en-

hanced precipitation (not shown here). Figure 2 displays the actual surface air temperature (SAT) along the ship cruise. The maximum SAT of  $28^{\circ}\text{C}$  is reached between  $20^{\circ}\text{N}$  and  $4^{\circ}\text{S}$ , except at the equator, where the air cools to a relative minimum of  $24^{\circ}\text{C}$  due to continuous rain fall.

Analysing sea level pressure (SLP) and wind measurements, the existing atmospheric circulation during the *TransBrom Sonne* cruise can be characterised (Fig. 3). The ship cruise starts within the climatological Westerlies followed by the northern trade wind regime. The lowest air pressure of the whole transit is recorded at the departure reaching 1003 hPa, due to the passage of Melor with strong Northwesterly winds. The air pressure then steadily increases up to 1017 hPa at  $34^{\circ}\text{N}$ . With the development and the approach of the tropical depression Nepartak on 8 October 2009, the air pressure suddenly drops south of  $30^{\circ}\text{N}$ . The maximum storm intensity hit the ship cruise on 12 October 2009 with 1007 hPa and a mean wind speed of  $19\text{ m s}^{-1}$  (in gusts reaching  $21\text{ m s}^{-1}$ ) from the Northeast (Fig. 3). The ship passes Nepartak on the northern to northeastern flank (Fig. 4). However, higher wind speeds occur on the northwestern flank, expecting in general enhanced emissions in this quadrant of the tropical depression. Two days later, the next tropical storm Lupit is reached at  $18^{\circ}\text{N}$  (Fig. 3). As it passes the ship route with a distance of more than 500 km (Fig. 1), the influence of Lupit on the ship measurements is weaker with strong Easterly winds of  $12\text{ m s}^{-1}$  and SLP of 1010 hPa. Probably due to its development into a super-typhoon, Lupit strongly influenced the oceanic methyl iodide entrainment into the stratosphere (Tegtmeier et al., 2013). After this storm event, air pressure and wind speed steadily decrease until crossing  $10^{\circ}\text{N}$ , when the wind speed starts to increase continuously (Fig. 3). We identify the inner tropical belt between  $12^{\circ}\text{N}$  and  $6^{\circ}\text{S}$  with a weak to moderate wind speed and a continuous left-hand rotation. South of  $6^{\circ}\text{S}$  intensifying southern trade winds begin to blow, exceeding  $16\text{ m s}^{-1}$  at  $12^{\circ}\text{S}$ . These stormy winds lead to an increase of evaporation, hence a cooling of the ocean surface within the South Equatorial Current (Fig. 2). Simultaneously with the SST decline, the SAT continuously decreases to  $23^{\circ}\text{C}$ . The air pressure starts to increase up to the absolute maximum of the cruise with 1018 hPa, finally arriving the end harbour in Townsville under high pressure influence (Fig. 3). The influence of the atmospheric tides on SLP appears southward of  $40^{\circ}\text{N}$ , clearly visible as semi-diurnal pressure variations with maximum amplitudes up to 4 hPa.

Figure 3 compares also two different meteorological assimilations, which are used as input for the trajectory calculations (Sect. 3), with the ship measurements. Overall, the data intercomparison for pressure and wind fields shows a good agreement, influenced by the assimilation of the radiosonde measurements as they were delivered to the GTS data net from the WMO. For air pressure and wind speed, the NCEP-GDAS analysis is in closer agreement with the ship measurements than opECMWF almost throughout the NH. South of

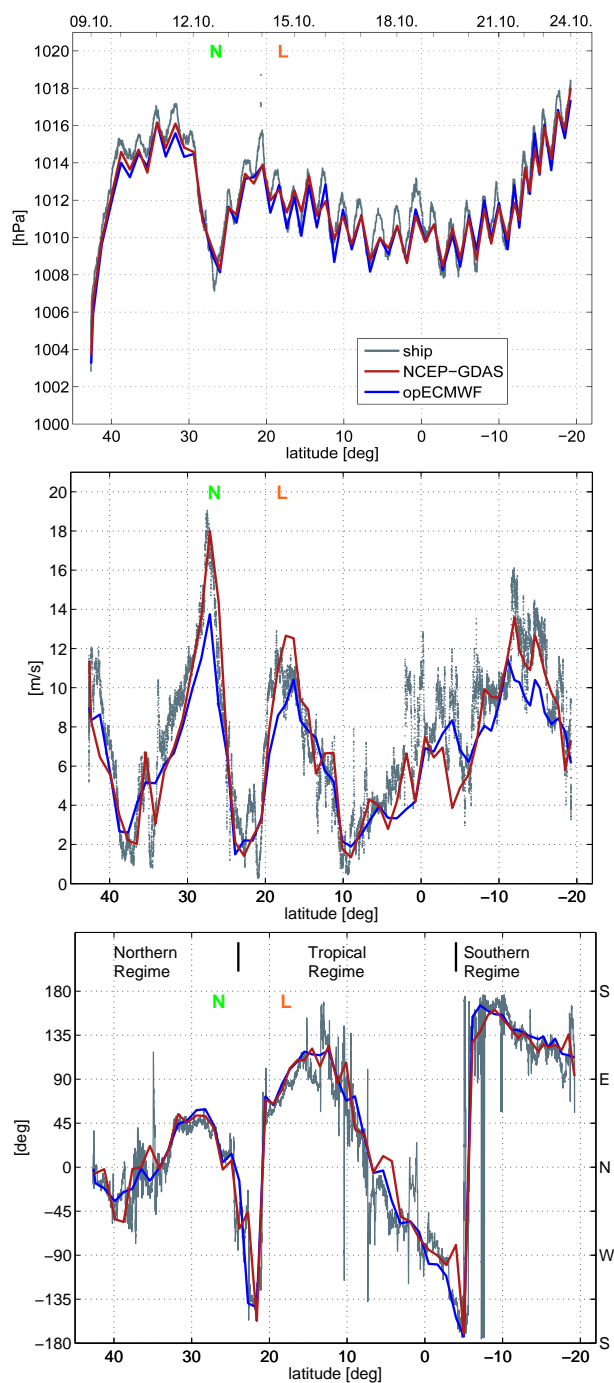


**Fig. 3.** Data intercomparison between ship measurements and two different data assimilations from: (Top) sea level pressure (hPa), (Middle) mean wind speed ( $\text{m s}^{-1}$ ), (Bottom) mean wind direction (in  $^{\circ}$  and compass direction) and atmospheric regimes during October 2009. The ship measurements are displayed as 10 min averages; the NCEP-GDAS (red lines) and opECMWF (blue lines) data at 6 hourly intervals.

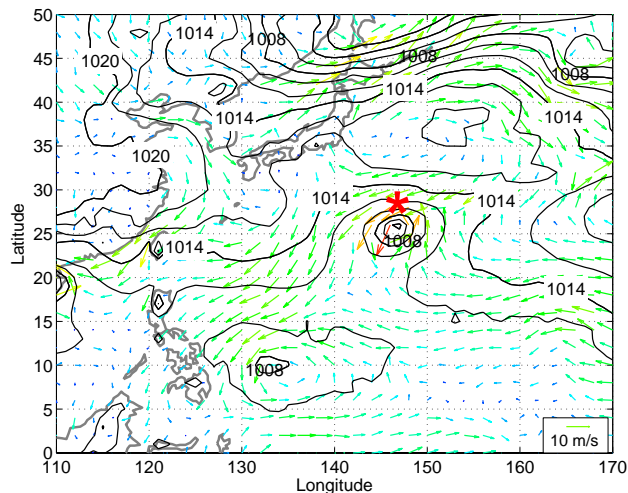


**Fig. 4.** Sea level pressure (hPa) and wind arrows ( $\text{m s}^{-1}$ ) for the storm Nepartak on 12 October 2009 at 12:00 UTC, using opECMWF analysis. The location of R/V *Sonne* is displayed by the red star. The contour intervals are 2 hPa.

the equator the differences increase, revealing a bias towards lower wind speeds of  $\sim 2\text{--}6 \text{ m s}^{-1}$  for both assimilation systems in the data sparser hemisphere probably due to lower coverage of mainland observations.

### 3 Analyses of air mass origin

To analyse air mass origin and possible source regions of the trace gases, two different trajectory models are employed, which are commonly used for trace gas analyses (Quack et al., 2004; Immler et al., 2007; Brinckmann et al., 2012; Ridder et al., 2012). The online web version of the Hybrid Single Particle Lagrangian Integrated Trajectory (HYSPLIT) model was applied (<http://ready.arl.noaa.gov/HYSPLIT.php>) using the NCEP-GDAS meteorological assimilation. The British Atmospheric Data Centre (BADC) trajectories were calculated online at the BADC trajectory service (<http://badc.nerc.ac.uk>) using the available opECMWF analyses with a  $1.125^{\circ} \times 1.125^{\circ}$  grid resolution. Both trajectory models were started daily at 12:00 UTC along the ship track within the MABL at 500 m altitude and 950 hPa for HYSPLIT respectively BADC, calculating 5-days backward. Trajectories started near the surface at 10 m height reveal qualitatively the same source areas (not shown here).

Figure 5 displays a clear separation into three atmospheric regimes for both trajectory analyses, which is in good agreement with the meteorological ship measurements (Fig. 3). The first regime, including the stronger Northerly winds, reaches until  $\sim 24^{\circ}$  N. The second regime with inner tropical characteristics, shows weaker winds (shorter trajectory length) and a rotation of the trajectories. At  $6^{\circ}$  S the air masses start to origin from the southeast distinguishing the

third regime with the climatological moderate to strong trade winds. Based on meteorological factors and air mass sources together (Figs. 3 and 5), the atmospheric circulation during the *TransBrom Sonne* cruise can be classified into three regimes: (1) the “Northern Regime” from 42° N to 24° N; (2) the “Tropical Regime” from 24° N to 6° S; and (3) the “Southern Regime” from 6° S to 19° S.

#### 4 *TransBrom Sonne* results

Given the starting points from the 5-day backward trajectories (Fig. 5), we can identify a variety of halocarbon source regions for the atmosphere. In the first regime, the air masses originate from East Russian and Japanese mainland and coastal areas. This air crosses the open ocean during the following days, where high biological productivity at the coast and in the open sea east of Japan was determined from in-situ measurements of chlorophyll *a* (Zindler et al., 2013). The atmosphere up to the North Equatorial Current contained anthropogenic, terrestrial and coastal properties, as well as an additional signature from oceanic phytoplankton (Quack et al., 2011; Zindler et al., 2013). Within the Tropical Regime, the air masses originate from more nearby areas, indicating the direct influence of open ocean sources on the atmosphere and its content of trace gases. Within the Southern Regime the trajectories pass Southeast Australia, the Tasman, Coral and Solomon Seas as well as the Great Barrier Reef. These regions comprise islands, coasts, coral reefs and high primary productivity (Zindler et al., 2013) as sources for the oceanic and atmospheric trace gas content (Quack et al., 2011).

Figure 6 shows the first measurements of bromoform concentrations in sea surface water along the meridional transect through the West Pacific. Elevated bromoform concentrations  $> 10 \text{ pmol L}^{-1}$  were found close to tropical islands ( $< 20 \text{ nm}$  distance, between 8° N and 4° S), in the Solomon Sea and within the Great Barrier Reef. The varying halocarbon concentrations are reflected by the above trajectory analyses. Higher atmospheric abundances, i.e.  $> 1 \text{ ppt}$  bromoform, were detected within the Northern and Southern Regimes (Quack et al., 2011; Brinckmann et al., 2012). Iodine monoxide (IO) was above detection limit, in contrast to bromine monoxide (BrO), and exceeded mixing ratios of 1 to 2 ppt within the Tropical Regime (Großmann et al., 2013). However, organic iodine precursors also measured in situ on-board of the *TransBrom* cruise were not sufficient to photochemically model the observed IO abundances, hinting towards a missing inorganic iodine source. Within the warm pool, extremely low ozone ( $\text{O}_3$ ) concentrations were detected during the *TransBrom* cruise by ozone sondes, Fourier Transform Infrared Spectroscopy (FTIR) and satellite measurements in the free troposphere (Ridder et al., 2012), leading to the conclusion that the OH shield must have “a hole” above the tropical West Pacific (Rex et al., 2012). These extremely

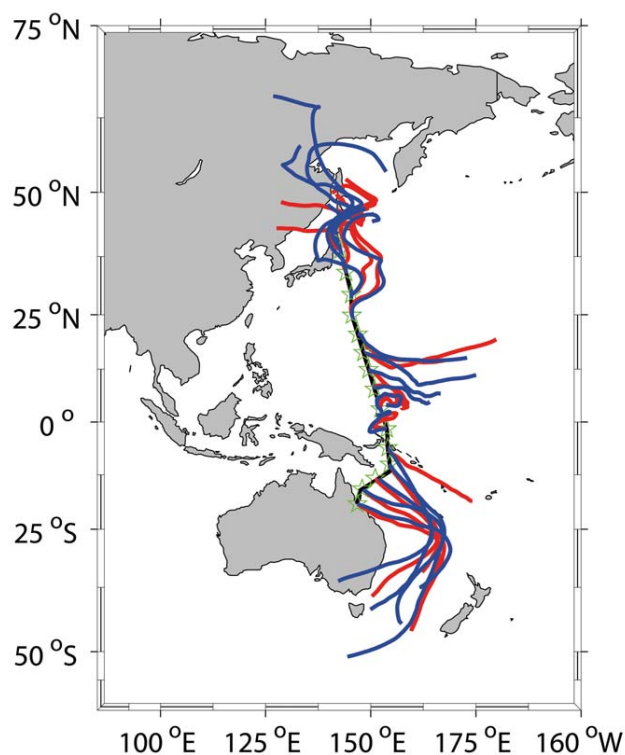


**Fig. 5.** 5-day backward trajectories calculated with the HYSPLIT (NCEP-GDAS data, red lines) and BADC (opECMWF 1.125° × 1.125° data, blue lines) models, started daily at 00:00 UTC along the cruise track, and at 500 m altitude and 950 hPa pressure level, respectively.

low OH values induce longer life and residence times of trace gases, increasing the chance of VSLS entrainment into the stratosphere.

Oceanic and atmospheric halocarbon measurements from *TransBrom* contributed to the global emission climatology for bromoform, dibromomethane and methyl iodide by Ziska et al. (2013). In-situ emissions from the *TransBrom* cruise yielded up to 50 % higher values than those from the climatological fields in this region. Using the in-situ bromocarbon emissions, Tegtmeier et al. (2012) estimated a bromine contribution up to 2.3 pptv to the stratosphere, when taking the combined source gas and product gas injections from bromoform and dibromomethane into the stratosphere into account. The corresponding maximum ODP values were projected to reach 6.4 and 4.1 for one unit of emitted oceanic bromoform and dibromomethane, respectively. Global high resolution trajectory calculations for the very short lived methyl iodide and DMS compounds revealed a significant amount to be delivered to the TTL, in good agreement with available aircraft measurements (Tegtmeier et al., 2013; Marandino et al., 2013). These two studies highlighted the potential of VSLS delivery to the stratosphere especially above the

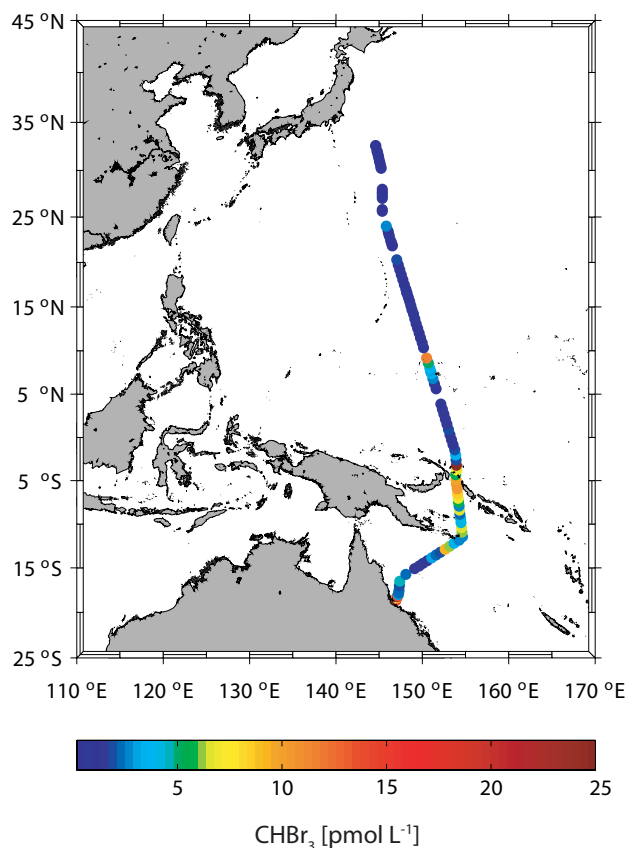


**Fig. 6.** Oceanic bromoform concentrations ( $\text{pmol L}^{-1}$ ) along the *TransBrom Sonne* cruise track during October 2009; measurement intervals are 3-hourly.

tropical West Pacific, where currently a lack of upper TTL and lower stratosphere in-situ measurements exists.

## 5 Conclusions

The *TransBrom Sonne* cruise through the tropical West Pacific took place in October 2009, during the typhoon season and a strengthening El Niño. Regular chemical, physical and biological measurements of air and sea water were conducted in order to analyse the distribution of halocarbons and other marine trace gases, their sources and their participation in atmospheric chemical processes. Anthropogenic and natural sources contributed to the variable marine and atmospheric trace gas concentrations within five oceanic and three atmospheric regimes, the “Northern”, “Tropical” and “Southern” regimes. The northern part of the extratropical and the tropical West Pacific was influenced by tropical storm and typhoon activity. Over the central part of the tropical West Pacific higher convective activity was observed, being typical for a strengthening El Niño phase. The climatological wind regime of strong southern trade winds was encountered south of  $6^\circ\text{S}$ . Based on trajectory predictions, we identified

populated and coastal source regions for trace gases in the northern part of the extratropical West Pacific and remote and coastal regions in the southern part of the tropical West Pacific. Open ocean air from the northern and central tropical West Pacific dominated the air masses during the middle leg of the cruise.

Overall, the *TransBrom Sonne* cruise delivered an unique data set of halocarbons and other ozone and climate relevant trace gases from the tropical West Pacific including both the surface ocean and the atmosphere, which are presented in this Atmospheric Chemistry and Physics special issue and elsewhere. Radiative and chemically active trace gases from the tropical West Pacific have an impact on the composition and chemistry of the tropical troposphere and stratosphere, potentially influencing the climate on a global scale. The halocarbon measurements and chemical transport modelling revealed that the tropical West Pacific is a significant source region for bromine and iodine emissions to the stratosphere during high convective and tropical storm activities.

*Acknowledgements.* We are grateful to all participants from *TransBrom Sonne* for their extensive work and help, which built the basis for the successful operation of the ship cruise. We thank Sebastian Wache, Steffen Fuhlbrügge and Helmke Hepach for the preparation of the figures. Data were provided from R/V *Sonne* for the ship measurements, from European Centre for Medium Range Weather Forecast for the operational ECMWF analysis and from National Centre for Environmental Prediction for the NCEP-GDAS analyses. This study was funded by the national WGL project TransBrom ([www.geomar.de/~transbrom](http://www.geomar.de/~transbrom)); the ship campaign on R/V *Sonne* was financed by the BMBF through grant 03G0731A. This work also contributes to the European Union’s Seventh Framework Programme FP7/2007-2013 under grant agreement no. 226224 – SHIVA.

The service charges for this open access publication have been covered by a Research Centre of the Helmholtz Association.

Edited by: K. Kreher

## References

- Bonazzola, M. and Haynes, P.: A trajectory-based study of the tropical tropopause region, *J. Geophys. Res.*, 109, D20112, doi:10.1029/2003JD004356, 2004.
- Brinckmann, S., Engel, A., Bönnisch, H., Quack, B., and Atlas, E.: Short-lived brominated hydrocarbons – observations in the source regions and the tropical tropopause layer, *Atmos. Chem. Phys.*, 12, 1213–1228, doi:10.5194/acp-12-1213-2012, 2012.
- Butler, J. H., King, D. B., Lobert, J. M., Montzka, S. A., Yvon-Lewis, S. A., Hall, B. D., Warwick, N. J., Mondeel, D. J., Aydin, M., and Elkins, J. W.: Oceanic distributions and emissions of short-lived halocarbons, *Global Biogeochem. Cy.*, 21, GB1023, doi:10.1029/2006GB002732, 2007.

- Fueglistaler, S., Bonazzola, M., Haynes, P. H., and Peter, T.: Stratospheric water vapor predicted from the Lagrangian temperature history of air entering the stratosphere in the tropics, *J. Geophys. Res.*, 110, D08107, doi:10.1029/2004JD005516, 2005.
- Gottelman, A., Salby, M. L., and Sassi, F.: Distribution and influence of convection in the tropical tropopause region, *J. Geophys. Res.*, 107, 4080, doi:10.1029/2001JD001048, 2002.
- Großmann, K., Frieß, U., Peters, E., Wittrock, F., Lampel, J., Yilmaz, S., Tschirner, J., Sommariva, R., von Glasow, R., Quack, B., Krüger, K., Pfeilsticker, K., and Platt, U.: Iodine monoxide in the Western Pacific marine boundary layer, *Atmos. Chem. Phys.*, 13, 3363–3378, doi:10.5194/acp-13-3363-2013, 2013.
- Hossaini, R., Mantle, H., Chipperfield, M. P., Montzka, S. A., Hamer, P., Ziska, F., Quack, B., Krüger, K., Tegtmeier, S., Atlas, E., Sala, S., Engel, A., Bönnisch, H., Keber, T., Oram, D., Mills, G., Ordóñez, C., Saiz-Lopez, A., Warwick, N., Liang, Q., Feng, W., Moore, F., Miller, B. R., Maréchal, V., Richards, N. A. D., Dorf, M., and Pfeilsticker, K.: Evaluating global emission inventories of biogenic bromocarbons, *Atmos. Chem. Phys. Discuss.*, 13, 12485–12539, doi:10.5194/acpd-13-12485-2013, 2013.
- Immler, F., Krüger, K., Tegtmeier, S., Fujiwara, M., Fortuin, P., Verver, G., and Schrems, O.: Cirrus clouds, humidity, and dehydration in the tropical tropopause layer observed at Paramaribo/Suriname (5.8N, 55.2W), *J. Geophys. Res.*, 112, D03209, doi:10.1029/2006JD007440, 2007.
- Krüger, K., Tegtmeier, S., and Rex, M.: Long-term climatology of air mass transport through the Tropical Tropopause Layer (TTL) during NH winter, *Atmos. Chem. Phys.*, 8, 813–823, doi:10.5194/acp-8-813-2008, 2008.
- Krüger, K., Tegtmeier, S., and Rex, M.: Variability of residence time in the Tropical Tropopause Layer during Northern Hemisphere winter, *Atmos. Chem. Phys.*, 9, 6717–6725, doi:10.5194/acp-9-6717-2009, 2009.
- Liu, C., Zipser, E. J., and Nesbitt, S. W.: Global Distribution of Tropical Deep Convection: Different Perspectives from TRMM Infrared and Radar Data, *J. Climate*, 20, 489–503, 2007.
- Marandino, C. A., Tegtmeier, S., Krüger, K., Zindler, C., Atlas, E. L., Moore, F., and Bange, H. W.: Dimethylsulphide (DMS) emissions from the western Pacific Ocean: a potential marine source for stratospheric sulphur?, *Atmos. Chem. Phys.*, 13, 8427–8437, doi:10.5194/acp-13-8427-2013, 2013.
- Montzka, S., Reimann, S., O'Doherty, S., Engel, A., Krüger, K., and Sturges, W. T.: Chapter 1: Ozone-Depleting Substances (ODSs) and Related Chemicals, "Scientific Assessment of Ozone Depletion: 2010", World Meteorological Organization, Geneva, Switzerland, 112 pp., 2011.
- Nightingale, P. D., Malin, G., Law, C. S., Watson, A. J., Liss, P. S., Liddicoat, M. I., Boutin, J., and Upstill-Goddard, R. C.: In situ evaluation of air-sea gas exchange parameterizations using novel conservative and volatile tracers, *Global Biogeochem. Cy.*, 14, 373–387, 2000.
- Peters, E., Wittrock, F., Großmann, K., Frieß, U., Richter, A., and Burrows, J. P.: Formaldehyde and nitrogen dioxide over the remote western Pacific Ocean: SCIAMACHY and GOME-2 validation using ship-based MAX-DOAS observations, *Atmos. Chem. Phys.*, 12, 11179–11197, doi:10.5194/acp-12-11179-2012, 2012.
- Quack, B. and Wallace, D. W. R.: Air-sea flux of bromoform: Controls, rates, and implications, *Global Biogeochem. Cy.*, 17, 1023, doi:10.1029/2002GB001890, 2003.
- Quack, B., Atlas, E., Petrick, G., Stroud, V., Schaufli, S., and Wallace, D. W. R.: Oceanic bromoform sources for the tropical atmosphere, *Geophys. Res. Lett.*, 31, L23S05, doi:10.1029/2004GL020597, 2004.
- Quack, B., Krüger, K., Atlas, E., Tegtmeier, S., Großmann, K., Rex, M., von Glasow, R., Sommariva, R., and Wallace, D.: Halocarbon sources and emissions over the Western Pacific, oral presentation on 05.04.2011, EGU, Vienna, Austria, 2011.
- Rex, M., Ridder, T., Notholt, J., Immler, F., Lehmann, R., Krüger, K., Mohr, V., and Tegtmeier, S.: Is there a hole in the global OH shield over the tropical Western Pacific warm pool?, *Quadrennial Ozone Symposium* (oral presentation on 28.12.2012), Toronto, C6017, 2012.
- Ridder, T., Gerbig, C., Notholt, J., Rex, M., Schrems, O., Warneke, T., and Zhang, L.: Ship-borne FTIR measurements of CO and O<sub>3</sub> in the Western Pacific from 43° N to 35° S: an evaluation of the sources, *Atmos. Chem. Phys.*, 12, 815–828, doi:10.5194/acp-12-815-2012, 2012.
- Tegtmeier, S., Krüger, K., Quack, B., Atlas, E. L., Pisso, I., Stohl, A., and Yang, X.: Emission and transport of bromocarbons: from the West Pacific ocean into the stratosphere, *Atmos. Chem. Phys.*, 12, 10633–10648, doi:10.5194/acp-12-10633-2012, 2012.
- Tegtmeier, S., Krüger, K., Quack, B., Atlas, E., Blake, D. R., Boenisch, H., Engel, A., Hepach, H., Hossaini, R., Navarro, M. A., Raimund, S., Sala, S., Shi, Q., and Ziska, F.: The contribution of oceanic methyl iodide to stratospheric iodine, *Atmos. Chem. Phys. Discuss.*, 13, 11427–11471, doi:10.5194/acpd-13-11427-2013, 2013.
- Wanninkhof, R.: Relationship between wind-speed and gas exchange over the ocean, *J. Geophys. Res.*, 97, 7373–7382, 1992.
- Yokouchi, Y., Li, H.-J., Machida, T., Aoki, S., and Akimoto, H.: Isoprene in the marine boundary layer (Southeast Asian Sea, eastern Indian Ocean, and Southern Ocean): Comparison with dimethyl sulfide and bromoform, *J. Geophys. Res.*, 104, 8067–8076, doi:10.1029/1998JD100013, 1999.
- Zindler, C., Bracher, A., Marandino, C. A., Taylor, B., Torrecilla, E., Kock, A., and Bange, H. W.: Sulphur compounds, methane, and phytoplankton: interactions along a north-south transit in the western Pacific Ocean, *Biogeosciences*, 10, 3297–3311, doi:10.5194/bg-10-3297-2013, 2013.
- Ziska, F., Quack, B., Abrahamsson, K., Archer, S. D., Atlas, E., Bell, T., Butler, J. H., Carpenter, L. J., Jones, C. E., Harris, N. R. P., Hepach, H., Heumann, K. G., Hughes, C., Kuss, J., Krüger, K., Liss, P., Moore, R. M., Orlikowska, A., Raimund, S., Reeves, C. E., Reifenhäuser, W., Robinson, A. D., Schall, C., Tanhua, T., Tegtmeier, S., Turner, S., Wang, L., Wallace, D., Williams, J., Yamamoto, H., Yvon-Lewis, S., and Yokouchi, Y.: Global sea-to-air flux climatology for bromoform, dibromomethane and methyl iodide, *Atmos. Chem. Phys.*, 13, 8915–8934, doi:10.5194/acp-13-8915-2013, 2013.